Conference materials
UDC 535.34:004.942
DOI: https://doi.org/10.18721/JPM.153.117

Radiation induced defects of zinc oxide particles with star and flower shapes

A. N. Dudin [1] ✉, V. I. Iurina [1], V. V. Neshchimenko [1], C. Li [2]

[1] Amur State University, Blagoveshchensk, Russia;
[2] Harbin Institute of Technology, Harbin, China
✉ andrew.n.dudin@gmail.com

Abstract: The paper presents the results of modeling a proton beam with energies of 100 keV on zinc oxide particles, with star and flower shapes, in the Geant4 software package. A high ability to accumulate primary defects was demonstrated for star-type particles in comparison with flower-type particles. A comparative analysis of the calculated data on the study of defects as a result of modeling with experimental data is carried out.

Keywords: zinc oxide, flower-shaped particles, star-shaped particles, degradation, radiation resistance, defects, protons, irradiation

Funding: The study was supported by the Ministry of Science and Higher Education of the Russian Federation № 122082600014-6.

Citation: Dudin A. N., Iurina V. I., Neshchimenko V. V., Li C., Radiation induced defects of zinc oxide particles with star and flower shapes. St. Petersburg State Polytechnical University Journal. Physics and Mathematics. 15 (3.1) (2022) 101–106. DOI: https://doi.org/10.18721/JPM.153.117

Материалы конференции
УДК 535.34:004.942
DOI: https://doi.org/10.18721/JPM.153.117

Радиационные дефекты частиц оксида цинка в форме звезды и цветка

А. Н. Дудин [1] ✉, В. Ю. Юрина [1], В. В. Нещименко [1], Ч. Ли [2]

[1] Амурский государственный университет, г. Благовещенск, Россия;
[2] Харбинский технологический университет, г. Харбин, Китай
✉ andrew.n.dudin@gmail.com

Аннотация. Представлены результаты моделирования пучка протонов с энергиями 100 кэВ на частицах оксида цинка в форме звезды и цветка в программном комплексе Geant4. Продемонстрирована высокая способность к накоплению первичных дефектов для частиц звездчатого типа по сравнению с частицами цветочного типа. Проведен сравнительный анализ расчетных данных по исследованию дефектов в результате моделирования с экспериментальными данными.

Ключевые слова: оксид цинка, частицы в форме цветка, частицы в форме звезды, деградация, радиационная стойкость, дефекты, протоны, облучение

Финансирование: Исследование выполнено при поддержке Министерства науки и высшего образования Российской Федерации № 122082600014-6.

Ссылка при цитировании: Дудин А. Н., Юрина В. Ю., Нещименко В. В., Ли Ч. Радиационные дефекты частиц оксида цинка в форме звезды и цветка // Научно-технические ведомости СПбГПУ. Физико-математические науки. 2022. Т. 15. № 3.1. С. 101–106. DOI: https://doi.org/10.18721/ JPM.153.117

Introduction

ZnO is a versatile semiconductor with excellent optical and electrical properties. The presence of a relatively large band gap and binding energy, combined with high optical stability when irradiated with charged particles, makes it promising for use in the space environment as thermal control coatings.

However, with prolonged exposure to sunlight quanta and ionizing study, a number of radiation defects and color centers are formed in zinc oxide grains [1–2]. This leads to degradation of optical properties due to absorption in the ultraviolet and visible regions, as well as to an increase in solar absorption. Therefore, it is important to investigate the effects of morphology on the behavior of the degradation of optical properties and related radiation defects.

Nanostructured particles have a number of differences from bulk materials: an increase in the specific surface of particles, as well as non-stoichiometry and high free surface energy, which provides a driving force for the diffusion of defects; structural distortions caused by size determine the stability of nanostructures; quantum limitation associated with electronic characteristics. The balance of the above properties and the concentration of point defects determine the stability of the optical properties under the action of ionizing radiation.

Studies of the radiation resistance and optical properties of pigments in thermal control coatings based on the direct-gap semiconductor II-IV of the semiconductor group ZnO have shown that the particle morphology plays an important role in the accumulation of radiation defects [3–4]. Therefore, we set ourselves the goal of comparing the resistance of ZnO particles with the 'star' and 'flower' form factors to the effects of low-energy protons, using both a model approach and a direct experimental one.

Materials and Methods

All chemicals used in this experiment were of analytical grade without purification.

Star-type particles were synthesized by the following method [5]: 0.9 mmol of $Zn(CH_3COO)_2 \cdot 2H_2O$ was dissolved in 1 mol of deionized water under magnetic stirring, then 14 mol of NH_4OH (25% aqueous solution) was added, after which 5.5 mmol of KBH_4 was added, continuing mixing. The solution was labeled in a Teflon lined autoclave. The closed autoclave was kept at 140°C for 8 hours. The autoclave was then cooled to room temperature naturally. The white product was collected without centrifugation and washed successively several times with deionized water and ethanol. The solution was dried in air at 60 °C without heat treatment.

To obtain flower type particles, 1 mol of deionized water and 1 mol of ethanol were mixed with 4 mmol of $Zn(CH_3COO)_2 \cdot 2H_2O$, followed by the addition of 25 mmol of NH_4HCO_3 and 0.8 mmol of γ-methacryloxypropyltrimethoxysilane. The solution was poured into a Teflon-coated autoclave, which was kept at 100° C for 6 hours. After cooling, the autoclave was opened, the white product was collected and washed successively several times with deionized water and ethanol. Finally, the thick solution was air dried at 60 °C and then heat treated at 650 °C for 3 hours.

The surface morphologies of the powders were analyzed by using a scanning electron microscope (SEM) Helios NanoLab 600i. The specific surface area of the powder was determined by the Brunauer–Emmet–Teller (BET) method with physical adsorption of nitrogen using an AutoSorb 6iSA technique.

Modeling was carried out in the GEANT4 software package, the star-type target geometry is a set of 13 cylinders 0.25 μm in diameter, crossed with each other, with a total swept diameter of 5 μm. The geometry of the flower-type target was half a sphere with a radius of 3 μm with segments of spheres included in it, forming petals with a thickness of 0.05 μm. The particles under consideration were packed into an ensemble sized 35×35×14 μm for star type particles, 36×36×9 μm for flower type particles.

Irradiation was carried out relative to the normal to the target surface by a monoenergetic proton beam with an energy of 100 keV and a fluence of 5×109 cm^{-2}. The threshold displacement energy for the zinc atom was chosen to be 52 eV, and 57 eV for the oxygen one [6].

When modeling, the processes used in the QGSP_BIG_EMY physics set were taken into

account, including: ionization of the medium, multiple scattering, elastic and inelastic scattering of hadrons, bremsstrahlung, etc.

The Frenkel defect concentration calculated in GEANT4 was determined using the modified Kinchin-Pisa formula [7]:

$$FP \sim \frac{E_{dis}}{2.5E_d}, \quad (1)$$

where E_d is the threshold displacement energy, E_{dis} is the dissipated energy in nuclear collisions.

Samples were tested using the Space Environment Simulator, which was composed of a system of vacuum pumps, chamber 0.06 m^3 in useful volume, a source of electromagnetic solar radiation, electron and proton Van de Graaff accelerators, and an in situ optical reflectance measurement system. The samples were irradiated by protons with an energy of 100 keV fluence 5×10^{15} cm^{-2} with a flux of 5×10^{11} $cm^{-2}s^{-1}$ in vacuum 2.5×10^{-4} Pa, while the initial vacuum was 5× 10×5 Pa.

The comparison was made with synthesized ZnO star and flower particles obtained by the hydrothermal method described above.

Results and Discussion

The SEM micrographs of synthesized particles are presented in Fig. 1. Star-type particles have a hierarchical structure with an average size of about 4 − 7 μm and consist of a radial arrangement of hundreds of nanorods. Flower-type particles with a size of 4 − 8 μm have rounded shapes, consisting of sheets located in an arbitrary direction. The yield of star and flower type particles is about 80%. The resulting nanostructured particles are micron in size, but consist of nanoparticles; accordingly, such particles have a combination of properties at the micro- and nanoscales. The average specific surface area measured by the BET method is 44.3 ± 2.9 m^2g^{-1} for star-type particles and 68.4 ± 6.6 m^2g^{-1} for flower-type particles.

a) *b*)

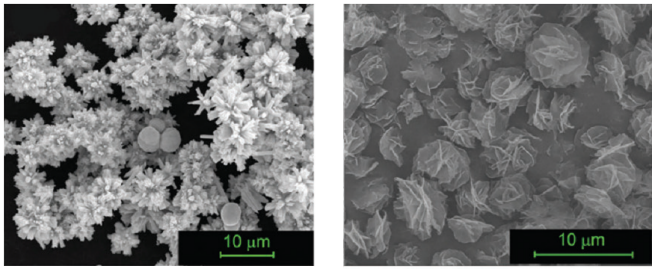

Fig. 1. SEM images of star (*a*) and flower (*b*) ZnO particles

The process of a proton beam with an energy of 100 keV with a fluence of 5×10^9 cm^{-2} passing through particles of the star and flower type is visualized in Fig. 2 and 3, respectively.

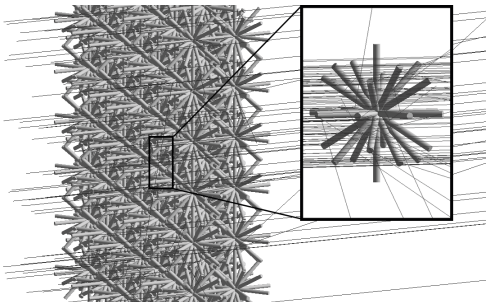

Fig. 2. Simulation in Geant4: zinc oxide particles star shape irradiated by protons

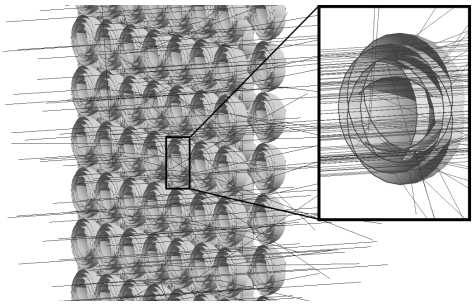

Fig. 3. Simulation in Geant4: zinc oxide particles flower shape irradiated by protons

Numerical calculations of the effect of radiation on a star-type particle give the proton mean free path equal to 1.41 Å The total number of primary knocked-on atoms (PKA) is 4.7×10^6 cm^{-3}. Concentration of formed primary defects (Frenkel pairs) is 1.88×10^{17} cm^{-3}. These parameters

take the following values for a flower-type particle: mean free path of 1.65 Å; PKA of 1.3×10^6 cm^{-3}; concentration of primary defects of 4.82×10^{16} cm^{-3}.

The reflectance spectra of the synthesized particles (Fig. 4) show a close match of the main absorption edge. The diffuse reflection coefficient before ($\rho_{\lambda0}$) and after irradiation ($\rho_{\lambda\phi}$) of flower-type particles is higher than that of star-type particles in the wavelength range from the edge of the main absorption to the near infrared (NIR) region. The difference between the spectra of synthesized particles in the near infrared region of the spectrum is due to free electrons and chemisorbed gases.

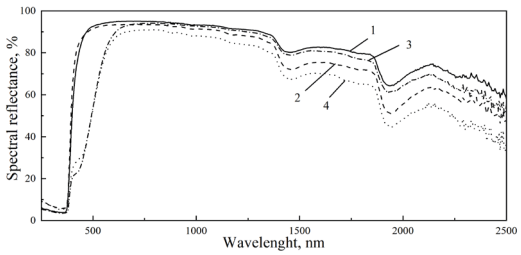

Fig. 4. Reflection spectra of synthesized particles before and after irradiation for flower (*1*, *3*) and star types (*2*, *4*)

The induced absorption spectra (Fig. 5) of the synthesized particles after irradiation with protons ($\Delta\rho_\lambda = \rho_{\lambda0} - \rho_{\lambda\Phi}$) show the main peak in the UV and visible spectral region. The induced absorption bands in the region from 350 to 630 nm of synthesized star and flower particles are similar in intensity and have a maximum value of 60%. As for the near-IR region, there is a decrease in the induced absorption spectrum for flower-type particles, in comparison with star-type particles. The difference in the intensity of the absorption bands in this region reaches 5%.

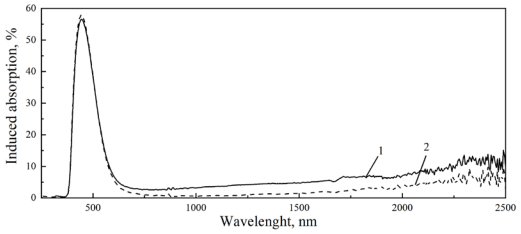

Fig. 5. Induced absorption spectra of synthesized particles for star (*1*) and flower (*2*) types

The ratio of intensities between different types of particles is associated with different concentrations of radiation defects Zn_i, V_{Zn}, O_i and V_O in different charge states, which are absorbed in different parts of the spectrum. The absorption of light quanta in the UV region is due to centers associated with Zn_i, but the absorption in the visible region of the spectrum with V_{Zn}, O_i, V_O and related complexes V_{Zn}-O_i and V_{Zn}-H, which is formed during implantation of hydrogen into the crystal lattice of ZnO. The absorption intensity in the near infrared region of the spectra after irradiation increases due to the Urbach tail.

The basic processes leading to the formation and accumulation of such defects are denoted as follows: Zn_{Zn}^X, O_O^X refer to atoms of zinc and oxygen in the lattice; $Zn_i^{\cdot\cdot}$, $Zn_i^{\cdot}$, $V_{Zn}^{''}$, $V_{Zn}^{'}$, $O_i^{''}$, $O_i^{'}$, $V_O^{\cdot\cdot}$, $V_O^{\cdot}$ to interstitial ions and vacancies of oxygen and zinc in different charge states; (H•)*, H• correspond to accelerated and thermalized protons; e′, h• to electron and hole.

The formation and separation of charge carriers by irradiation with accelerated protons may occur during the reactions of the formation of interstitial zinc and oxygen:

$$Zn_{Zn}^X + O_O^X + (H^{\cdot})^* \rightarrow V_{Zn}^{'} + Zn_i^{\cdot\cdot} + O_O^X + H, \qquad (2)$$

$$V_{Zn}^{'} + Zn_i^{\bullet\bullet} \rightarrow V_{Zn}^{X} + Zn_i^{\bullet}, \quad (3)$$

$$Zn_{Zn}^{X} + O_O^{X} + (H^{\bullet})^{*} \rightarrow Zn_{Zn}^{X} + V_O^{\bullet\bullet} + O_i^{'} + H, \quad (4)$$

$$V_O^{\bullet\bullet} + O_O^{'} \leftrightarrow V_O^{\bullet} + O_i^{X}. \quad (5)$$

The numerous knocked-out atoms can induce the cascade of atomic collisions. As a result, no equilibrium and inhomogeneous distribution of point defects: in the center vacancies predominate, on the periphery—interstitial atoms. For nanostructured particles at high energies of impinging particles normally only a small part of the projectile energy is deposited onto the nanosystem, in contrast to the case of irradiation of bulk systems when all the energy is eventually dispersed in the sample [8]. The following stage is defect recovery, i.e., the mutual recombination of vacancies and interstitial atoms, resulting in both point defects disappearance. Other processes simultaneously occur, such as vacancies being captured by pores and dislocations of the unoccupied type, the interstitial atoms being absorbed by dislocations, and the association of vacancies with complexes.

The numerous knocked-out atoms can induce the cascade of atomic collisions. As a result, no equilibrium and inhomogeneous distribution of point defects: in the center vacancies predominate, on the periphery—interstitial atoms. For nanostructured particles at high energies of impinging particles normally only a small part of the projectile energy is deposited onto the nanosystem, in contrast to the case of irradiation of bulk systems when all the energy is eventually dispersed in the sample [8]. The following stage is defect recovery, i.e., the mutual recombination of vacancies and interstitial atoms, resulting in both point defects disappearance. Other processes simultaneously occur, such as vacancies being captured by pores and dislocations of the unoccupied type, the interstitial atoms being absorbed by dislocations, and the association of vacancies with complexes.

Thermalized hydrogen and oxygen can diffuse from the lattice to the pigment surface with the subsequent desorption. The remaining defects after this stage are stable to exist for a long time. These defects will further define optical properties of a pigment. These peaks can be attributed to the surface molecules oxygen or hydrogen, or its association with lattice cation vacancies such as (V_{Zn}-H) [8].

Thermalized protons can interact with zinc vacancies or interstitial oxygen:

$$V_{Zn}^{'} + H_i \rightarrow V_{Zn}^{X} + H_i^{'}. \quad (6)$$

The process of release begins with the surface oxygen and subsequently the oxygen in the lattice, which is then accompanied by appearance of anion vacancies and interstitial zinc in differently charged states. The molecular oxygen reaction can occur in the vacuum volume:

$$2O_O + Zn_{Zn} \leftrightarrow Zn_i^{\bullet\bullet} + 2e^{'} + O_2, \quad (7)$$

$$O_O^{X} \leftrightarrow V_O^{\bullet\bullet} + 2e^{'} + \frac{1}{2}O_2, \quad (8)$$

$$O_2 \leftrightarrow 2O_O + V_{Zn}^{''} + 2h^{\bullet}. \quad (9)$$

Conclusion

It has been established that ZnO particles of the flower type have a higher radiation resistance to the action of protons compared to ZnO particles of the star type This is indicated by the calculated values obtained in the simulation, which demonstrate a higher concentration of primary defects for star-type particles, i.e., 1.88×10^{17} cm^3 compared to 4.82×10^{16} cm^{-3} for flower-type particles. The synthesized flower-shaped particles have a higher reflectivity, which indicates a lower concentration of intrinsic pre-radiation defects, which, in turn, can become one of the factors determining a lower concentration of radiation defects compared to star-shaped particles. The induced absorption spectra of synthesized particles demonstrate a high concentration of induced defects for star-type particles, which directly correlates with the data obtained from the simulation. To summarize, we can conclude that ZnO particles of the flower type are more radiation-resistant to the effects of protons compared to ZnO particles of the star type.

REFERENCES

1. **Mikhailov M. M., Dvoretskii M. I.,** Analysis of diffuse reflection and absorption spectra of ZnO in the near-IR region, Sov. Phys. J. 31 (1988) 591–594.

2. **Li C., Lv J., Yao S., Hu J., Liang Z.,** Study of the degradation and recovery of the optical properties of H+-implanted ZnO pigments, Nucl. Instrum. Methods Phys. Res., Sect. B. 295 (2013) 11–15.

3. **Flores N. M., Pal U., Galeazzi R., Sandoval A.,** Effects of morphology, surface area, and defect content on the photocatalytic dye degradation performance of ZnO nanostructures, RSC Advances. 4 (77) (2014) 41099–41110.

4. **Dudin A. N., Neshchimenko V. V., Yurina V. Y.,** Radiation defects induced by proton exposure in hollow zinc-oxide particles, Journal of Surface Investigation: X-Ray, Synchrotron and Neutron Techniques. 14 (4) (2020) 823–829.

5. **Li L., Yang H., Qi G., Ma J., Xie X., Zhao H., Gao F.,** Synthesis and photoluminescence of hollow microspheres constructed with ZnO nanorods by H2 bubble templates, Chemical Physics Letters. 455 (1-3) (2008) 93–97.

6. **Lorenz K., Alves E., Wendler E., Bilani O., Wesch W., Hayes M.,** Damage formation and annealing at low temperatures in ion implanted ZnO, Applied Physics Letters. 87 (19) (2005) 191904–191906.

7. **Leroy C., Rancoita P. G.,** Principles of radiation interaction in matter and detection, 2nd Edition, World Scientific Publishing Co. 2016.

8. **Brauer G., Anwand W., Grambole D., Grenzer J., Skorupa W., Čížek J., Kuriplach J., Procházka I., Ling C.C., So C.K., Schulz D., and Klimm D.,** Identification of Zn-vacancy-hydrogen complexes in ZnO single crystals: A challenge to positron annihilation spectroscopy, Physical Review B. 79 (11) (2009) 115212–115227.

THE AUTHORS

DUDIN Andrey N.
andrew.n.dudin@gmail.com
ORCID: 0000-0002-4791-6353

NESHCHIMENKO Vitaly V.
v1ta1y@mail.ru
ORCID: 0000-0002-5559-4876

IURINA Viktoria I.
viktoriay-09@mail.ru
ORCID: 0000-0003-3611-9495

LI Chundong
lichundong@hit.edu.cn
ORCID: 0000-0003-2546-6395

Received 19.05.2022. Approved after reviewing 19.07.2022. Accepted 20.07.2022.